



**HAL**  
open science

## Experimental characterization of the icephobic surfaces properties for optimization of ice slurry production

Walid Samah, Pascal Clain, Francois Rioual, Laurence Fournaison, Anthony Delahaye

### ► To cite this version:

Walid Samah, Pascal Clain, Francois Rioual, Laurence Fournaison, Anthony Delahaye. Experimental characterization of the icephobic surfaces properties for optimization of ice slurry production. 26e Congrès International du Froid (International Congress of Refrigeration 2023 "ICR 2023"), Institut International du Froid (IIF), Aug 2023, Paris France, France. 10.18462/iir.icr.2023.0211 . hal-04193075

**HAL Id: hal-04193075**

**<https://hal.inrae.fr/hal-04193075v1>**

Submitted on 3 Oct 2023

**HAL** is a multi-disciplinary open access archive for the deposit and dissemination of scientific research documents, whether they are published or not. The documents may come from teaching and research institutions in France or abroad, or from public or private research centers.

L'archive ouverte pluridisciplinaire **HAL**, est destinée au dépôt et à la diffusion de documents scientifiques de niveau recherche, publiés ou non, émanant des établissements d'enseignement et de recherche français ou étrangers, des laboratoires publics ou privés.

# Experimental characterization of the icephobic surfaces properties for optimization of ice slurry production

Walid SAMAH<sup>\*(a,b)</sup>, Pascal CLAIN<sup>(a,b)</sup>, François RIOUAL<sup>(b)</sup>, Laurence FOURNAISON<sup>(b)</sup>, Anthony DELAHAYE<sup>(b)</sup>

<sup>(a)</sup>Leonard de Vinci Pôle Universitaire, Research Center, 92916 Paris La Défense, France.

<sup>(b)</sup>Université Paris-Saclay, INRAE, FRISE, 92761 Antony, France.

\*Corresponding author: walid.samah@inrae.fr

## ABSTRACT

In the refrigeration industry, ice slurries are an alternative to reduce the use of refrigerants with high greenhouse gas content. However, the production of these ice slurries requires the use of scraped surface generators. These generators have high maintenance costs due to the wear of the scrapers caused by the ice adhering to the generator walls and consume additional mechanical energy. Because of these drawbacks, it is important to study the icephobic behavior of surfaces to find alternatives that significantly reduce ice adhesion without consuming additional energy. Our study consists in experimentally characterizing the icephobic behavior of different types of surfaces and in studying the detachment of ice from the surfaces by flow. The objective is to understand the phenomena behind ice adhesion to select icephobic surfaces. The final goal is to design an ice slurry generator without mechanical scraping.

Keywords: Secondary refrigeration, Ice slurry generator, Ice slurry, Phase change materials (PCM), Ice adhesion, Hydro-scraping.

## 1. INTRODUCTION

The production of cold using refrigerants can have negative consequences for the environment and human health. Therefore, there is a growing interest in developing innovative sustainable and energy-efficient refrigeration production and transport techniques. Secondary refrigeration is a method of reducing the amount of refrigerant used in conventional systems by limiting their use to cold production, while cold transport is provided by environmentally neutral fluids such as ice slurry or gas hydrate slurry (Samah et al., 2023a). Ice slurry-based cold transport is a crucial technology for the food industry, air conditioning, medical care and other industrial applications (Kauffeld et al., 2010). Ice slurry is defined as a mixture of ice particles suspended in an aqueous solution (solid-liquid mixture) with an average ice particle diameter of 1 mm ( $10^{-3}$  m) or less (Egolf and Kauffeld, 2005). Ice slurry has many advantages, such as a good management of electricity consumption thanks to its latent heat of fusion (storage) and a zero impact on the environment (Kauffeld et al., 2010). There are several ice slurry generators, either with moving components directly related to the ice extraction from the surface (Stamatiou et al., 2005), or without moving components (Samah et al., 2023a). Methods with moving components have disadvantages such as low energy efficiency (additional power consumption) and high maintenance costs or discontinuous ice slurry production. To overcome these limitations, new experimental approaches to ice slurry production without moving components have been developed to reduce ice adhesion: by using icephobic surfaces, hydro-scraping with reduced surface cooling energy, hydro scraping within Helical Coiled Heat Exchanger (HCHX) made of Nylon 11 or Polytetrafluoroethylene (Teflon<sup>®</sup> or PTFE) (Samah et al., 2023a). However, these experimental methods also have drawbacks. For example, the study of ice slurry production by hydro-scraping in the Helical Coiled Heat Exchanger (HCHX) (Brooks et al., 2021, 2020), and the study of ice slurry production by hydro-scraping (Barth, 2000) are carried out in compact exchangers which are not clear and do not allow visualization of ice detachment phenomena on the surface. These studies deserve to be deepened with the visualization of the

phenomena of tearing off the ice on the surface by the flow, that with variation of the velocity of flow and the surface states to better understand the ice adhesion phenomena.

This study aims to understand the phenomena of ice adhesion and extraction by flow (hydro scraping) to develop a method of ice slurry production without moving components (without mechanical scrapers). It also aims to understand the effect of surface condition and flow velocity on ice detachment to select the most optimal conditions. The originality of this study lies in the evaluation of the ice detachment length  $L_D$  along a surface as a function of the flow velocity and by visualizing the ice detachment phenomenon with a high-speed camera. For this purpose, three types of surfaces (hydrophilic, hydrophobic and superhydrophobic) were studied in a transparent rectangular box containing a 10 wt.% ethanol/water mixture.

## 2. MATERIALS AND METHODS

An experimental setup was developed to identify surfaces that allow optimal ice detachment by shear flow of a 10 wt.% ethanol/water mixture (crystallization temperature is  $-4.50\text{ }^\circ\text{C}$ ) through a nozzle generating a jet. The objective is to better understand the phenomena of ice adhesion and detachment on several types of surfaces to develop new ice slurry generators without moving components.

### 2.1. Experimental device of ice detachment study

To achieve this objective, a system is developed to allow the study of ice detachment by flow on several surfaces, this system is presented in figure 1. This system is composed of an aluminium heat exchanger (component 8 on figure 3). This exchanger is insulated on all 5 sides except the upper side on which the surface samples to be studied will be glued with thermal paste. This system also includes a flat nozzle with a rectangular outlet section  $S_N$  of  $0.03\text{ m} \times 0.002\text{ m}$  (component 9 on figure 3). The entire system is immersed in a 10 wt.% ethanol/water mixture with an immersion height between the top surface of the exchanger and the water interface of  $0.02\text{ m}$  ( $2\text{ cm}$ ). The ice detachment length  $L_D$  is defined as the maximum distance between the nozzle outlet section and the un-detached ice layer.

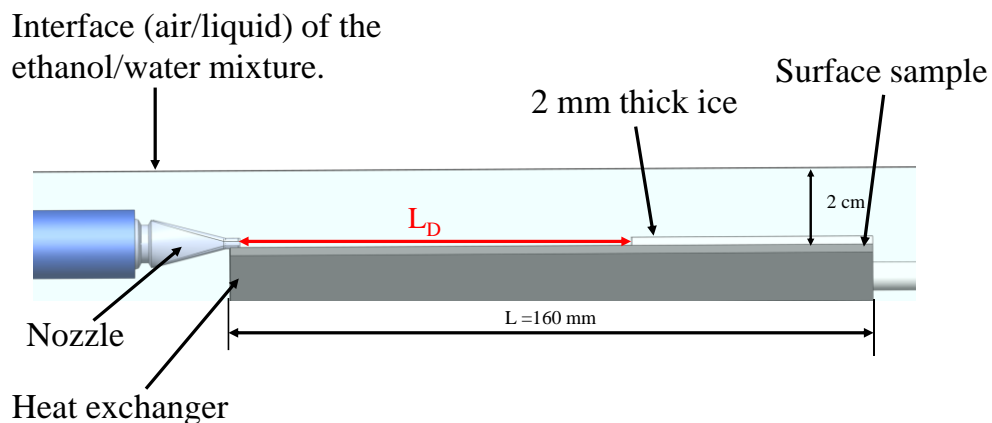


**Figure 1: Schematic representation of the system for studying ice detachment by flow.**

Three types of treated (superhydrophobic, hydrophobic) and untreated (hydrophilic) AW1050H24 aluminium surfaces are characterized to determine their icephobic behavior for the study of ice detachment by flow. The first surface is an untreated (hydrophilic) aluminium exhibiting an average contact angle (CA) (average between left and right contact angle) of  $58.21^\circ$  measured with an  $8.4\text{ }\mu\text{L}$  drop of a 10 wt.% ethanol/water mixture at an ambient temperature of  $23\text{ }^\circ\text{C}$ , as shown in Figure 2 (a). This surface forms an average contact angle of  $82.36^\circ$  with deionized water (Samah et al., 2023b). The second surface, aluminium, is treated by bonding a  $13\text{ }\mu\text{m}$  ( $1.3 \times 10^{-5}\text{ m}$ ) thick PTFE adhesive tape manufactured by REKALRO. This ribbon consists of a PTFE-coated fiberglass fabric, which provides additional properties of tear, tensile and puncture resistance. This surface is characterized by an average contact angle of  $91.38^\circ$  measured with an  $8.4\text{ }\mu\text{L}$  ( $8.4 \times 10^{-9}\text{ m}^3$ ) drop of a 10 wt.% ethanol/water mixture, as shown in Figure 2 (b). Teflon® (PTFE) is currently one of the best icephobic materials reducing ice adhesion strength due to its low dielectric permittivity of about  $\approx 2.1$

(Menini and Farzaneh, 2009), but its disadvantage is its low thermal conductivity. In our study case, the thickness is very small (13  $\mu\text{m}$  thick) to avoid heat transfer problems. The third surface of AW1050H24 aluminium is treated with a commercial superhydrophobic coating "Ultra Ever Dry" (UED) applied in two steps by spraying. A first coat (reference: 35808), is applied with a drying time of 50 minutes, followed by a second coat (reference: 35809) with a drying time of 15 minutes, after treatment, the average contact angle with deionized water is 157.59° in the Cassie state compared to that of the untreated surface which is 82.36° (Samah et al., 2023b). An average contact angle of 151.50° measured with an 8.4  $\mu\text{L}$  drop of a 10 wt.% ethanol/water mixture is shown in Figure 2 (c). This coating is already characterized in a previous study (Samah et al., 2023b).

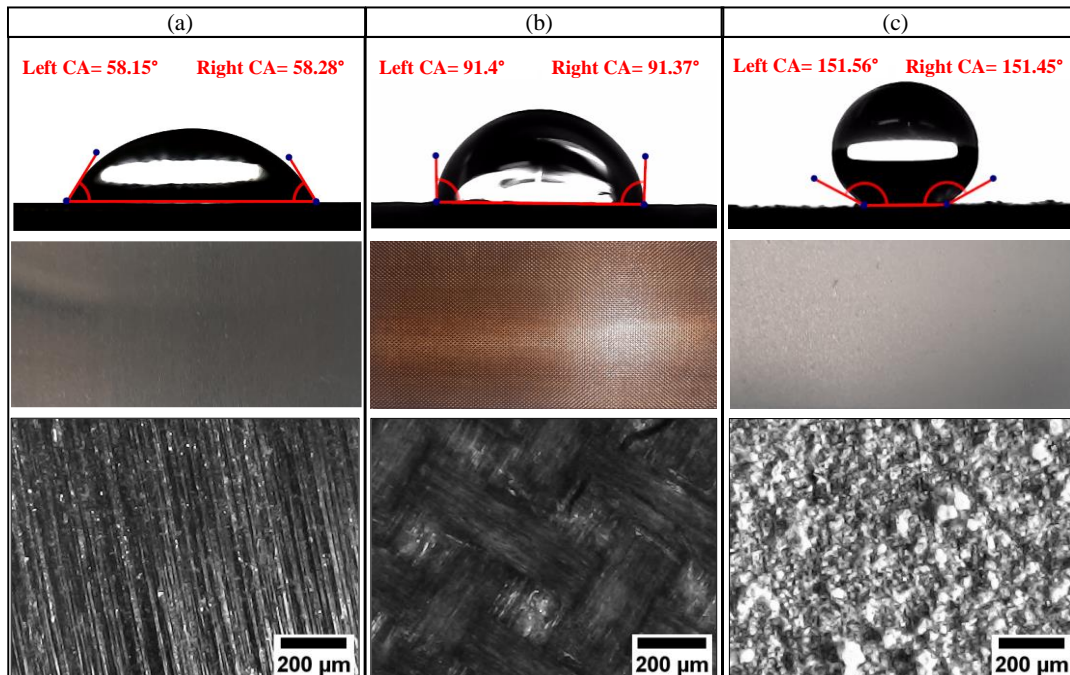


**Figure 2: Three types of surfaces studied: (a) hydrophilic "untreated aluminium"; (b) hydrophobic "aluminium treated with PTFE ribbon"; (c) superhydrophobic "aluminium treated with UED".**

To maintain the liquid level at 0.02 m (2 cm) between the studied surface and the air-liquid interface, the system shown in Figure 1 is placed in a transparent box (PMMA) (component 2 in Figure 3). This whole system is called surface testing section, it also consists of a high-speed camera (component 7) with a recording speed of 750 FPS. The video recording of the ice layer formation and its detachment by the flow is performed using the AOS Imaging Studio software version 4.7.2.4. The device also includes a second digital camera placed above the exchanger to take pictures after the ice detachment (component 1). The ice detachment length  $L_D$  is measured using IC Measure software version 2.0.0.286. A servo motor (component 15) equipped with a wiper (component 14) is installed to allow dew that forms on the surface of the PMMA box to be removed in the field of view of the high-speed camera during the cooling of the mixture to better visualize the formation and detachment of ice by flow. The servo motor is controlled by a controller board (component 3), programmed with C++ code to allow the wiper to make a round trip every 4 seconds with an opening angle of 120°. The nozzle is fed by a circulating cryostat (component III in Figure 4), with a variable mass flow rate, the maximum flow rate being up to 0.167  $\text{kg s}^{-1}$  (10  $\text{kg min}^{-1}$ ). Finally, the PMMA box is fed by a filling tube (component 12) with a mass flow rate of 0.151  $\text{kg s}^{-1}$  (9.08  $\text{kg min}^{-1}$ ), the box having an outlet to the circulating cryostat (component 6). The total mass of the liquid mixture in the experimental setup is  $M_l = 12 \text{ kg}$ .

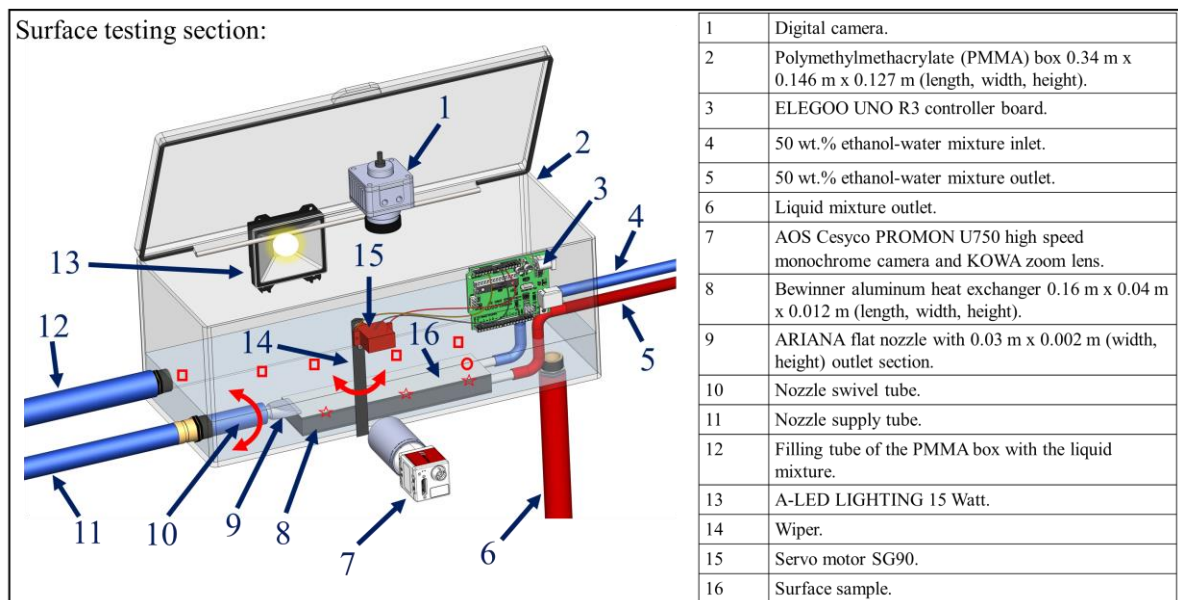


**Figure 3: Detailed schematic of surface testing section (component I in Figure 4).**

Five T-type thermocouples are placed on the surface testing section to measure the temperature of the mixture at different locations, represented in Figure 3 by red squares. Three T-type thermocouples are placed between the surface sample (component 16) and the heat exchanger (component 8), shown in Figure 3 by red stars. A thermocouple is placed on the surface sample 0.15 m (150 mm) from the nozzle outlet section, represented in Figure 3 by a red circle. The purpose of placing only one thermocouple on the sample surface is to minimize disturbance during ice formation and detachment. Tests were performed to verify the homogeneity of the temperature along the sample surface, and the result shows an average difference over several points that does not exceed  $\pm 0.5$  °C. This result validates the use of a single thermocouple on the surface. The measurement uncertainty of the thermocouples is  $\pm 0.028$ . The thermocouples are connected to a KEYSIGHT Model DAQ970A data acquisition system linked to a computer.

The complete experimental setup is shown in Figure 4 and consists of two JULABO circulating cryostats component II and component III, a Grundfos pump (component IV), an ABB Coriolis mass flow meter (component V) and a surface testing section to study the ice detachment on different surfaces (component I). The whole device is placed in a climate chamber set at 13 °C to improve the efficiency of the circulating cryostats.

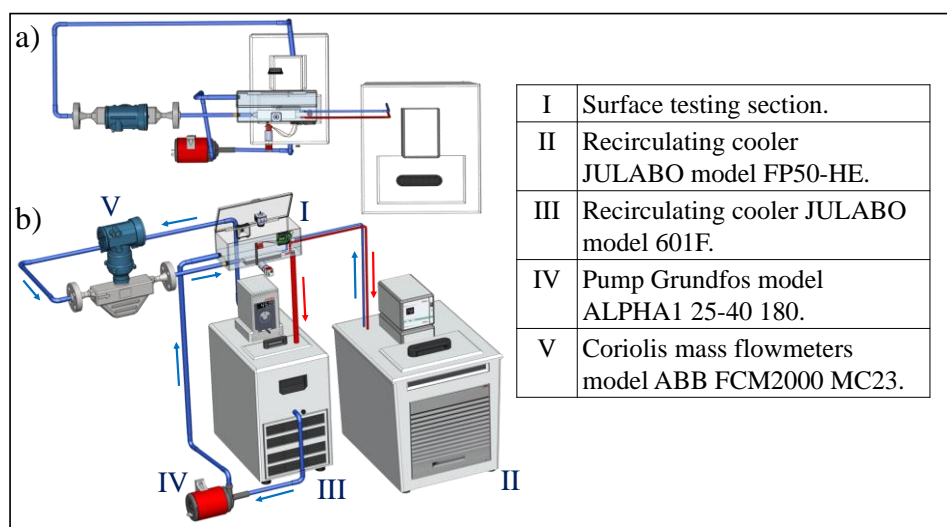


**Figure 4: Experimental setup to study ice detachment by flow on different surfaces with a 10 wt.% ethanol/water mixture.**

## 2.2. Experimental parameters and protocols

The objective of our study is to characterize the surfaces that have less adhesion to ice. Three types of surfaces (hydrophilic, hydrophobic, and superhydrophobic) are studied to form a 2 mm layer of ice in immersion, and then a jet of liquid is sent through the nozzle to detach the ice longitudinally on the surface to measure the ice detachment length  $L_D$  on each surface for different velocities. The variables in our experiments are surface states (hydrophilic, hydrophobic, and superhydrophobic) and jet velocities that range from 0 to  $2.84 \text{ m s}^{-1}$ . For all our flowing ice detachment experiments, surface temperatures are set to a target value of  $-8 \text{ }^\circ\text{C}$ . The experimental protocol is as follows: First, the filling pump (component IV in Figure 4) of the ice detachment study device is turned on and set to a power of 22 W to have a water level of 0.02 m above the heat exchanger (component 8 in Figure 3) thus a mass flow rate of  $0.151 \text{ kg s}^{-1}$ . Next, the temperature of the circulating cryostats (components III and II in Figure 4) that feed the heat exchanger and the surface test section, respectively, is set to an initial temperature of  $25 \text{ }^\circ\text{C}$ . Then, the temperature of both recirculating coolers is lowered to the desired value ( $-8 \text{ }^\circ\text{C}$ ) until a 2 mm (0.002 m) ice thickness is formed on the surface sample under investigation with a 10 wt.% ethanol/water mixture (the phase change temperature is between  $-4.5 \text{ }^\circ\text{C}$ ). Meanwhile, the nozzle (component 9 in Figure 3) is directed upward to maintain the flow of the aqueous mixture at a rate of  $0.025 \text{ kg s}^{-1}$  through the tube feeding the nozzle to avoid its heating before the ice detachment and not to disturb the formation of the ice layer on the surface sample (component 16 in Figure 3). Next, the flow of liquid through the nozzle is stopped, and the nozzle is directed toward the surface sample. Then, the mass flow rate through the nozzle is adjusted to the desired value, and the cryostat circulating pump (component III in Figure 4), which feeds the nozzle, is turned on for ice detachment by the flow of the aqueous mixture. Then, the filling pump (component IV in Figure 4) and the cryostat circulating pump (component III in Figure 4) are turned off when ice detachment is complete. Finally, a picture of the surface is taken with a camera (component 1 in Figure 3), and the detachment length ( $L_D$ ) is measured with the image processing software IC Measure version 2.0.0.286.

Figure 6 shows an example of the evolution of the mass flow rate through the nozzle and the temperature of the aqueous mixture (10 wt.% ethanol/water) and the untreated aluminium surface during cooling. The initial temperature of the mixture and the surface is  $25 \text{ }^\circ\text{C}$  and is lowered to  $-3.6 \text{ }^\circ\text{C}$  to achieve temperature stability. Then, the surface temperature is lowered to the target value of  $-8 \text{ }^\circ\text{C}$  to form a 2 mm ice layer, as shown in Figure 5. It takes about 310 seconds to achieve a 2 mm layer. The flow through the nozzle is stopped (step 1 in Figure 6), then the nozzle is directed downward (toward the surface) and a mass flow rate of  $0.109 \text{ kg s}^{-1}$  is initiated (corresponding to a flow velocity at the nozzle outlet of  $1.83 \text{ m s}^{-1}$ ), to remove the ice layer from the surface (step 2 in Figure 6). Finally, the flow is stopped when the ice layer is no longer removed from the surface (step 3 in Figure 6).

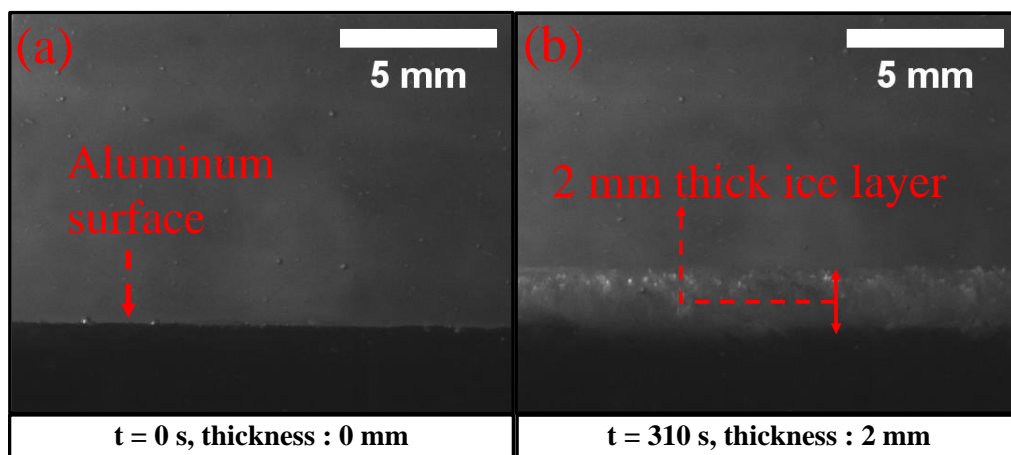
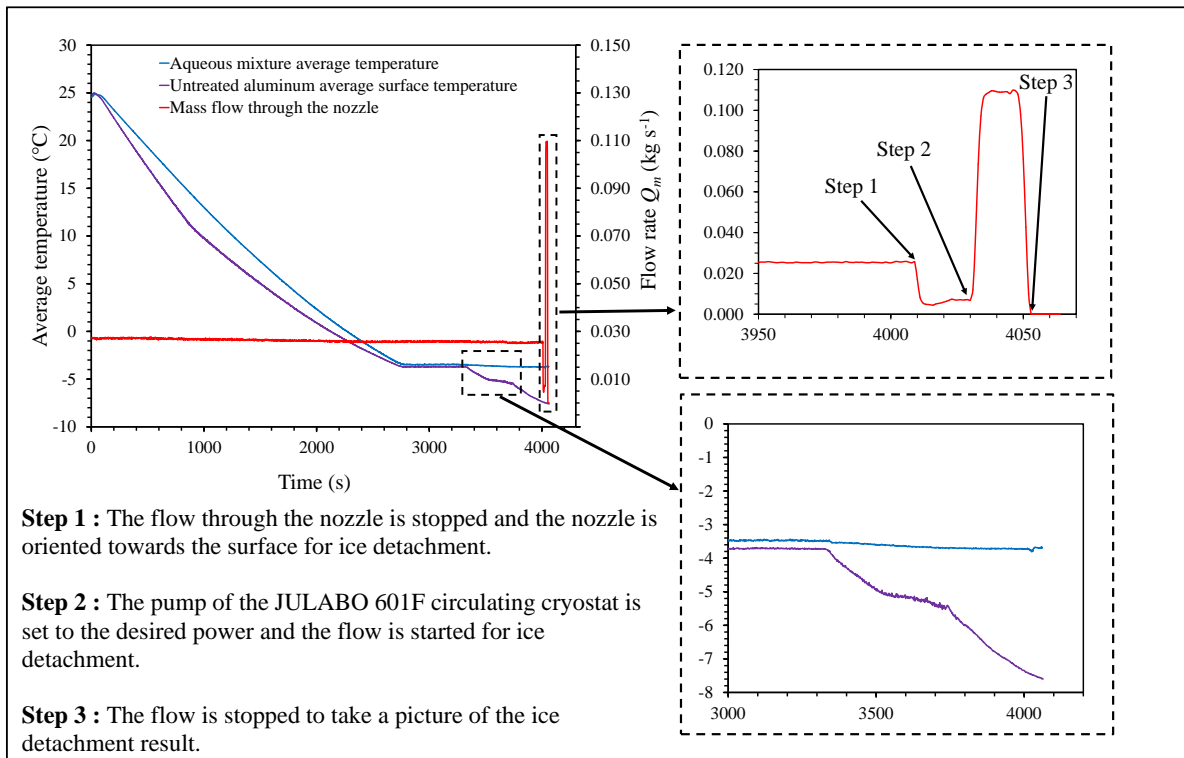


Figure 5: Evolution of the thickness of the ice layer that forms on an untreated aluminium surface in a 10 wt.% ethanol/water mixture at a set surface temperature of  $-8 \text{ }^\circ\text{C}$ , (a): before crystallization; (b): after crystallization.



**Figure 6:** Example of evolution of the mass flow rate through the nozzle and the average temperature of the aqueous mixture (10 wt.% ethanol/water mixture) and the average temperature of the untreated aluminium surface (hydrophilic) during the cooling process.

### 3. RESULTS AND DISCUSSIONS

#### 3.1. Ice detachment by flow on the three types of surfaces studied

Figure 7 shows the evolution of the ice detachment length  $L_D$  as a function of the average velocity of the aqueous mixture at the nozzle outlet, for the three types of surface samples studied: untreated aluminium "Al" (hydrophilic), aluminium treated with Teflon® adhesive ribbon "PTFE" (hydrophobic) and aluminium treated with Ultra Ever Dry coating "UED" (superhydrophobic). In our experiments, we calculated the flow velocity  $V_N$  at the nozzle outlet using the following relationship Eq. (1):

$$V_N = \frac{Q_m}{\rho_l S_N} \quad \text{Eq. (1)}$$

This relationship uses the following data: the mass flow rate  $Q_m$ , the density of the mixture  $\rho_l$  (equal to  $983.4 \text{ kg m}^{-3}$  at the liquid temperature  $T_l$  of  $-3.6 \text{ }^\circ\text{C}$ ), and the nozzle outlet cross-section  $S_N$  equal to  $6 \times 10^{-5} \text{ m}^2$ .

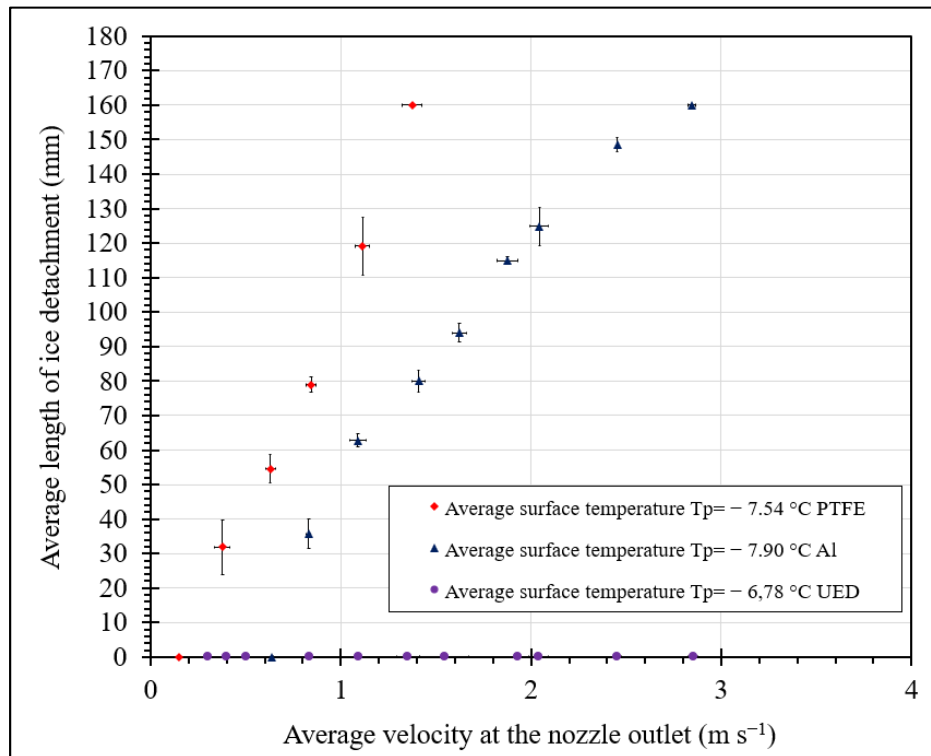


**Figure 7: Evolution of the ice detachment length as a function of the average velocity of the aqueous mixture at the nozzle outlet, for the three types of samples studied: untreated aluminium "Al" (hydrophilic), aluminium treated with a Teflon® ribbon "PTFE" (hydrophobic) and aluminium treated with the Ultra Ever Dry coating "UED" (superhydrophobic).**

In the experiments, the mass flow rate varies from 0 to 0.17 kg s<sup>-1</sup>. This implies a flow velocity ranging from 0 to 2.87 m s<sup>-1</sup>. Figure 7 shows that the ice does not detach from the aluminium surface treated with the UED superhydrophobic coating, for all the flow velocities studied. This is in agreement with existing research (Lei et al., 2021), as superhydrophobic surfaces are very rough and ice adhesion occurs by mechanical anchoring in the substrate asperities. The increase in surface roughness leads to an increase in the contact area and the number of potential anchoring sites (Zou et al., 2011). There are four mechanisms that can explain the phenomenon of ice adhering to a surface (Samah et al., 2023a): the mechanical mechanism, the chemical mechanism, the electrostatic mechanism, and the boundary layer mechanism (He et al., 2017; Landy and Freiberger, 1967; Lliboutry, 1964). For the untreated aluminium surface (hydrophilic), it is noticed that under a speed of 0.6 m s<sup>-1</sup>, no ice detachment is visible on the surface. Above this minimum speed of 0.6 m s<sup>-1</sup>, ice detachment becomes possible and the evolution of the detachment length  $L_D$  as a function of speed is linear. To detach all the ice along the 160 mm (0.16 m) exchanger, a speed of about 2.87 m s<sup>-1</sup> is required. Finally, for the aluminium surface treated with PTFE adhesive tape, the minimum ice detachment velocity on this surface is equal to 0.15 m s<sup>-1</sup>, which is four times less than the minimum detachment velocity on the untreated aluminium surface. To detach all the ice along the heat exchanger, a speed of about 1.37 m s<sup>-1</sup> is required, half that of the untreated aluminium surface. This shows that Teflon® has good icephobicity characteristics and low ice adhesion compared to the untreated aluminium surface (hydrophilic) and the UED treated aluminium surface (superhydrophobic). This result is in agreement with the results of (Brooks et al., 2021, 2020), and the results of ice adhesion tests on Teflon® (PTFE) of (Fillion et al., 2017). The use of a Teflon® (PTFE) coating or adhesive ribbon on the ice slurry generator will reduce the amount of energy required for ice detachment from the surface, provided that the Teflon® coating or adhesive ribbon is thin enough not to penalize heat transfer. The ice growth rate results show that ice growth is faster on the superhydrophobic surface due to its roughness which has more nucleation sites. Ice growth is slower on the smooth untreated aluminum surface due to its low roughness (fewer nucleation sites).



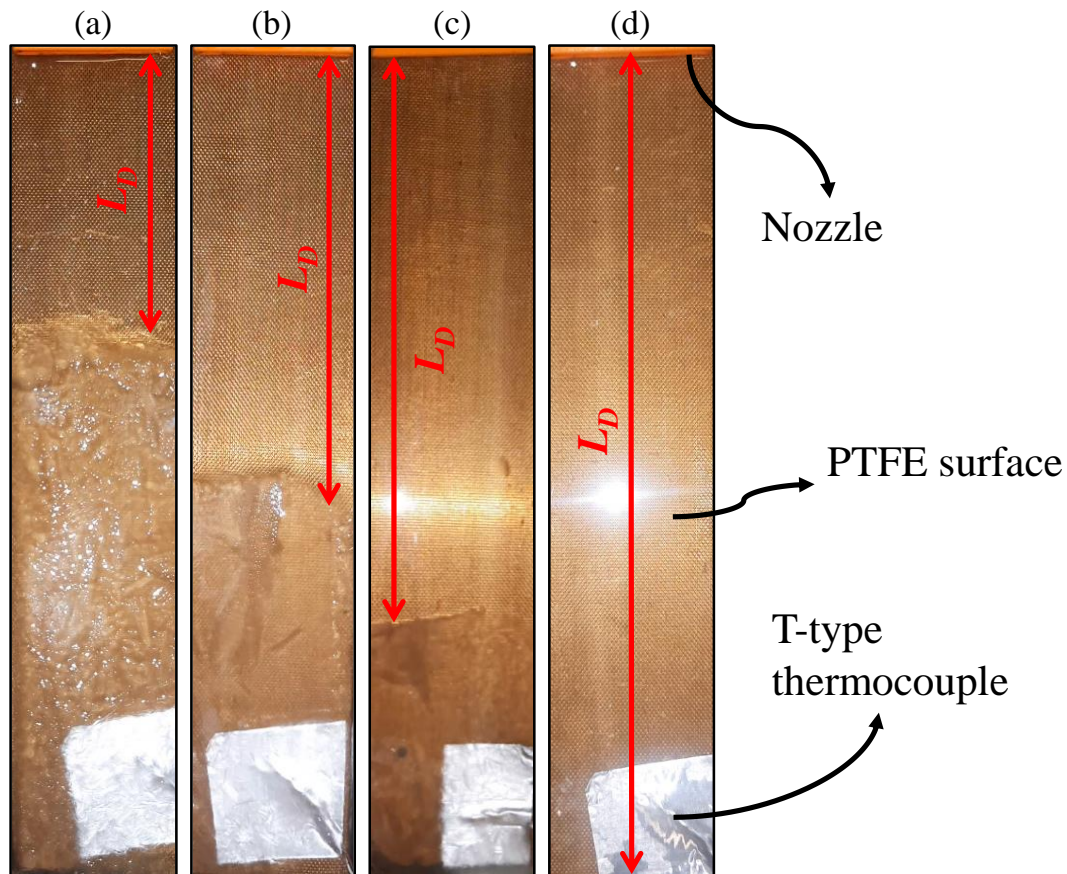


**Figure 8:** Example of the result of the detachment length " $L_D$ " (m) of the ice by flow for the case of an aluminium surface treated with the adhesive ribbon PTFE for an average surface temperature of  $-7.54\text{ }^{\circ}\text{C}$ : (a)  $V_N = 0.64\text{ m s}^{-1}$  and  $L_D = 0.057\text{ m}$ ; (b)  $V_N = 0.86\text{ m s}^{-1}$  and  $L_D = 0.08\text{ m}$ ; (c)  $V_N = 1.08\text{ m s}^{-1}$  and  $L_D = 0.113\text{ m}$ ; (d)  $V_N = 1.41\text{ m s}^{-1}$  and  $L_D = 0.16\text{ m}$ .

Figure 8 shows the results of ice detachment length  $L_D$  on an aluminium surface treated with Teflon (PTFE) adhesive ribbon for different flow velocities and an average surface temperature of  $-7.54\text{ }^{\circ}\text{C}$ . Ice detachment on this surface is by adhesive peeling, i.e., the ice is completely removed from the surface without leaving any residue, and the ice layer is soft (needle-like morphology), which allows the ice to disintegrate into particles under flow agitation. The reason for this soft ice texture is due to the presence of ethanol. The use of additives reduces the ice cohesion (Samah et al., 2023a). If pure water is used to produce the ice, it will have a hard texture and will come off the surface in one piece without disintegrating into particles (Samah et al., 2023b).

Figures 9 and 10 show the images of the ice detachment by flow on the aluminium surface treated with PTFE adhesive tape and on the aluminium surface treated with Ultra Ever Dry "UED" coating, respectively for a flow velocity of about  $2\text{ m s}^{-1}$ . It can be seen in Figure 9 that the ice detachment from the PTFE surface is adhesive, i.e., the entire ice layer detaches from the surface without leaving any ice residue on the surface. Then, the ice that detaches from this PTFE surface disintegrates into ice particles due to the presence of the additive (ethanol) that makes the ice layer soft during crystallization and flow detachment. It can be seen that after 1.35 seconds, the entire ice layer is detached from the PTFE surface. The ice detaches in the same way on the untreated aluminium surface.

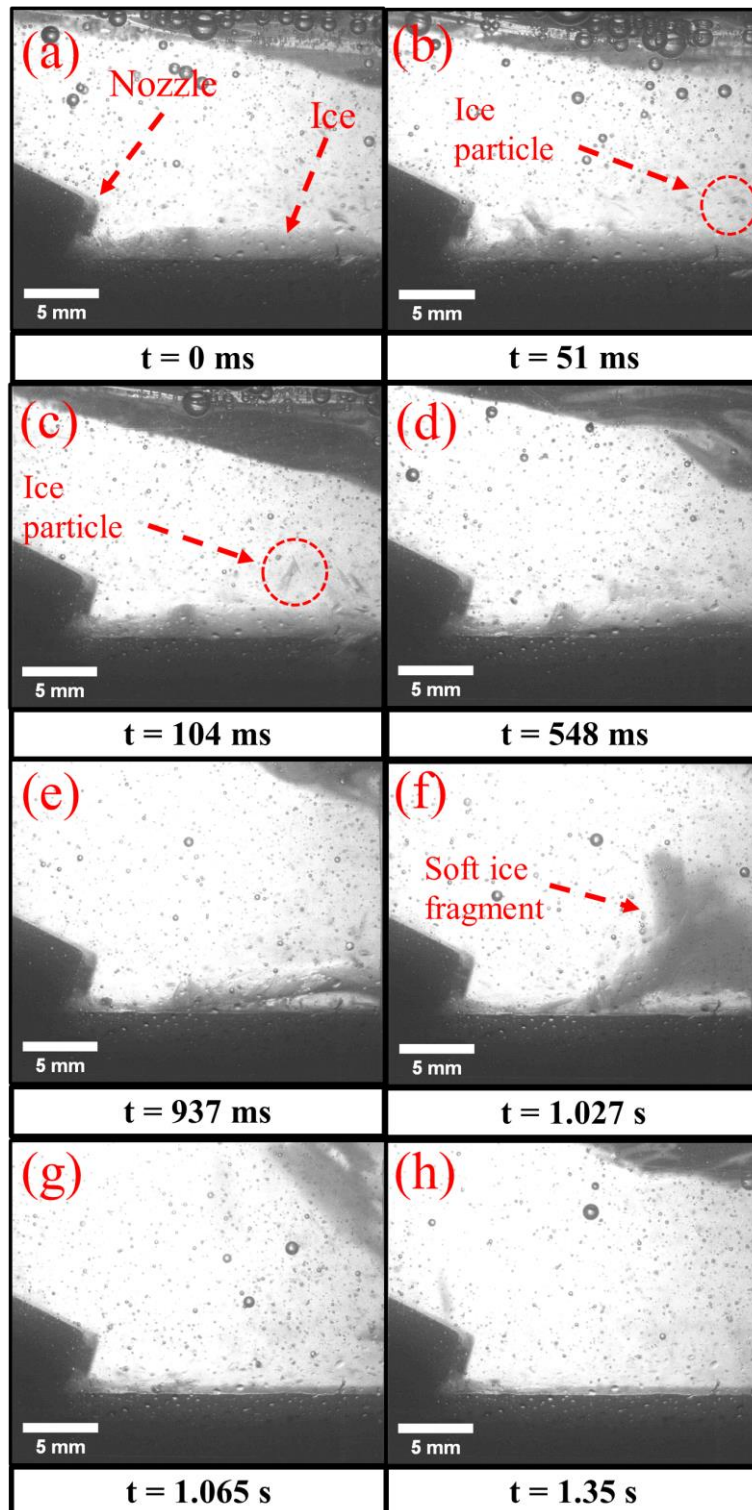


Figure 9: Illustration of ice detachment by flow on an aluminium surface treated with PTFE tape, for an average surface temperature of  $-7.54\text{ }^{\circ}\text{C}$ , a mass flow rate of  $0.13\text{ kg s}^{-1}$  ( $7.5\text{ kg min}^{-1}$ ) thus a nozzle outlet velocity of  $2.11\text{ m s}^{-1}$  for the 10 wt.% ethanol/water mixture.

For the aluminium surface treated with the UED superhydrophobic coating, the ice does not detach from the surface for all flow velocities studied (see Figure 7). This is due to the roughness of the superhydrophobic surface. However, after 9.9 seconds, a reduction in ice thickness is observed near the nozzle outlet due to the breakup of ice crystals in this ice layer (see Figure 10). Thus, this type of ice breakup is called cohesive detachment because the ice does not completely detach from the surface. The aluminium surface treated

with UED superhydrophobic coating has higher ice adhesion than the untreated aluminium surface treated with PTFE ribbon.

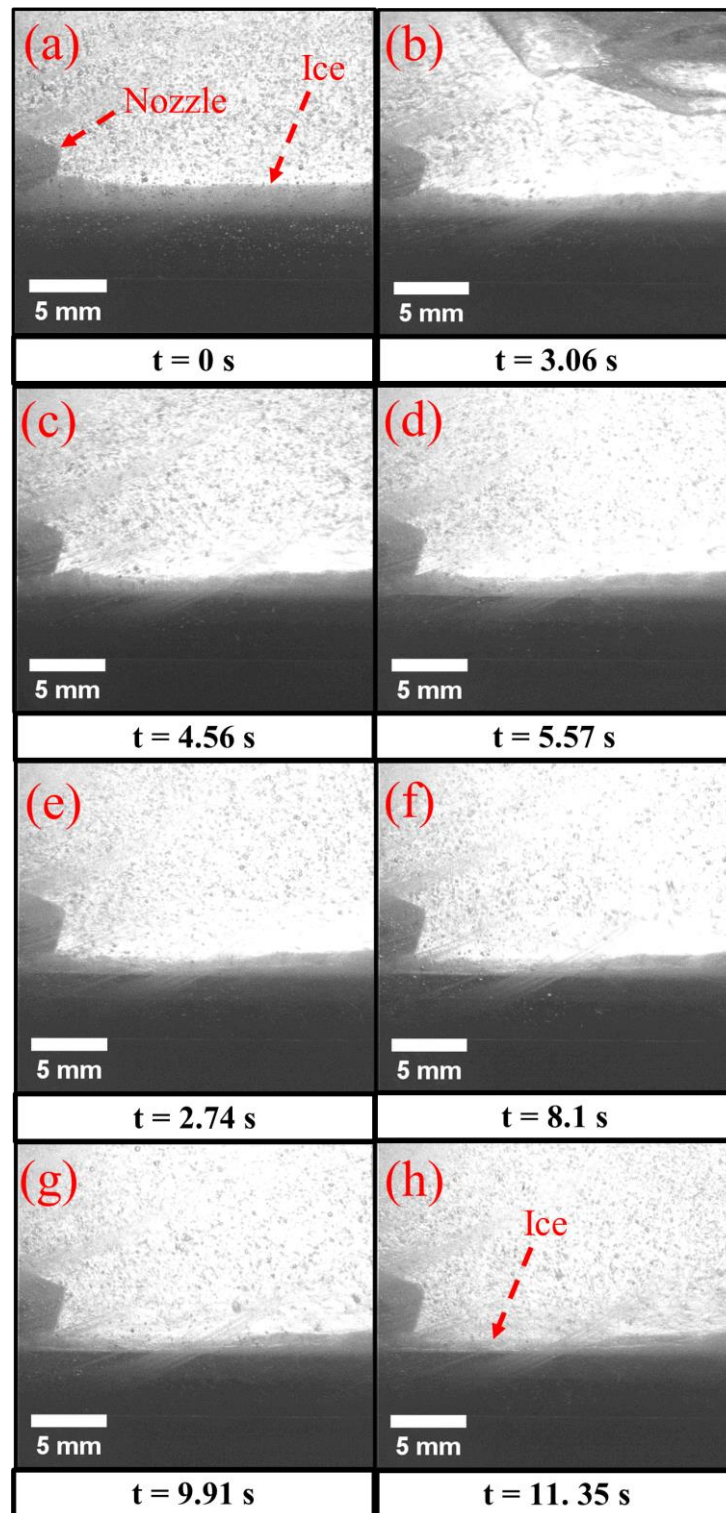


Figure 10: Illustration of ice detachment by flow on an aluminium surface treated with Ultra Ever Dry coating "UED", for an average surface temperature of  $-6.78\text{ }^{\circ}\text{C}$ , a mass flow rate of  $0.12\text{ kg s}^{-1}$  ( $7.11\text{ kg min}^{-1}$ ) thus a nozzle outlet velocity of  $2.01\text{ m s}^{-1}$  for the 10 wt.% ethanol/water mixture.

## 4. CONCLUSIONS

This study focused on understanding the mechanisms of ice adhesion and detachment by flow for ice slurry production, and for developing a method for ice slurry production without mechanical scrapers. It also examined the effect of surface condition and flow velocity for ice detachment to identify optimal conditions. The results showed that the ice adhesion is by mechanical adhesion (mechanical inking) on the aluminium surfaces treated with the UED superhydrophobic coating, due to the surface condition (rough surface) which is very different from the untreated aluminium surfaces and the surfaces treated with PTFE ribbon. In addition, the results indicated that a minimum flow velocity of  $0.6 \text{ m s}^{-1}$  is required for ice detachment on an untreated aluminium surface (hydrophilic), whereas a minimum flow velocity of  $0.15 \text{ m s}^{-1}$  is sufficient for ice detachment on an aluminium surface treated with PTFE adhesive tape. This indicates that PTFE has effective ice repelling properties and reduces ice adhesion compared to the untreated aluminium surface. The experiments revealed two distinct modes of ice detachment: adhesive detachment on surfaces with lower roughness (such as untreated aluminium surfaces and aluminium surfaces treated with PTFE adhesive ribbons), and cohesive detachment of the ice on surfaces with higher roughness, such as the aluminium surface treated with a UED superhydrophobic coating. In the case of cohesive detachment, the ice layer does not fully separate from the surface, but the crystals within the layer break apart. The use of a PTFE coating or adhesive ribbon on the ice slurry generator could reduce the energy required to remove ice from a surface.

## ACKNOWLEDGEMENTS

The authors would like to thank the National Research Institute for Agriculture, Food and the Environment and De Vinci Research Center for their financial support of ice slurry research.

## NOMENCLATURE

### **Symbols**

<i>L</i>	Length (m)
<i>M</i>	Mass (kg)
<i>Q</i>	Mass flow rate ( $\text{kg s}^{-1}$ )
<i>S</i>	Section ( $\text{m}^2$ )
<i>T</i>	Temperature ( $^{\circ}\text{C}$ )
<i>V</i>	Velocity ( $\text{m s}^{-1}$ )
<b>Greek</b>	
$\rho$	Density ( $\text{kg m}^{-3}$ )

### **Subscripts**

<i>D</i>	Detachment
<i>l</i>	Liquid
<i>N</i>	Nozzle

### **Abbreviations**

CA	Contact angle
UED	Ultra Ever Dry
PTFE	Polytetrafluoroethylene
PMMA	Polymethylmethacrylate

## REFERENCES

- Barth, M., 2000. Procède pour detacher les cristaux de glace d'un échangeur thermique generateur d'un frigoporteur diphasique liquide-solide. EP1101071B1.
- Brooks, S., Quarini, G., Tierney, M., Yun, X., Lucas, E., 2020. Conditions for continuous ice slurry generation in a nylon helical coiled heat exchanger. *Therm. Sci. Eng. Prog.*, 15, 100427.
- Brooks, S., Tierney, M., Quarini, G., 2021. Experimental investigation of different materials for use in ice slurry generation. *Int. J. Refrig.*, 129, 97–108.
- Egolf, P.W., Kauffeld, M., 2005. From physical properties of ice slurries to industrial ice slurry applications. *Int. J. Refrig.*, 28(1), 4–12.
- Fillion, R.M., Riahi, A.R., Edrissy, A., 2017. Design factors for reducing ice adhesion. *J. Adhes. Sci. Technol.*, 31(21), 2271–2284.
- He, Z., Xiao, S., Gao, H., He, J., Zhang, Z., 2017. Multiscale crack initiator promoted super-low ice adhesion surfaces. *Soft Matter*, 13(37), 6562–6568.
- Kauffeld, M., Wang, M.J., Goldstein, V., Kasza, K.E., 2010. Ice slurry applications. *Int. J. Refrig.*, 33(8), 1491–1505.
- Landy, M., Freiberger, A., 1967. Studies of ice adhesion: I. Adhesion of ice to plastics. *J. Colloid Interface Sci.*, 25(2), 231–244.

- Lei, S., Fang, X., Ou, J., Wang, F., Xue, M., Li, W., Amirfazli, A., Chini, S.F., 2021. Icing of static and high-speed water droplets on superhydrophobic surface. *Mater. Lett.*, 285, 129048.
- Lliboutry, L., 1964. The crystalline texture and plastic deformation of ice. *J. Hydraul. Res.*, 2(1), 41–49.
- Menini, R., Farzaneh, M., 2009. Elaboration of Al<sub>2</sub>O<sub>3</sub>/PTFE icephobic coatings for protecting aluminium surfaces. *Surf. Coat. Technol.*, 203(14), 1941–1946.
- Samah, W., Clain, P., Rioual, F., Fournaison, L., Delahaye, A., 2023a. Review on ice crystallization and adhesion to optimize ice slurry generators without moving components. *Appl. Therm. Eng.*, 119974.
- Samah, W., Clain, P., Rioual, F., Fournaison, L., Delahaye, A., 2023b. Experimental investigation on the wetting behavior of a superhydrophobic surface under controlled temperature and humidity. *Colloids Surf. Physicochem. Eng. Asp.*, 656, 130451.
- Stamatiou, E., Meewisse, J.W., Kawaji, M., 2005. Ice slurry generation involving moving parts. *Int. J. Refrig.*, 28(1), 60–72.
- Zou, M., Beckford, S., Wei, R., Ellis, C., Hatton, G., Miller, M.A., 2011. Effects of surface roughness and energy on ice adhesion strength. *Appl. Surf. Sci.*, 257(8), 3786–3792.